Multi-scale crack closure measurements with digital image correlation on Haynes 230

Stefano Beretta, Silvio Rabbolini, Angelo Di Bello

Department of Mechanical Engineering, Politecnico di Milano
stefano.beretta@polimi.it, silvio.rabbolini@polimi.it, angelo1.dibello@mail.polimi.it

ABSTRACT. An experimental campaign was developed to study fatigue crack growth in Haynes 230, a Ni-based superalloy. The effects of crack closure were investigated with digital image correlation, by applying two different approaches. Initially, full field regression algorithms were applied to extract the effective stress intensity factor ranges from the singular displacement field measured at crack tips. Local closure measurements were then performed by considering crack flanks relative displacements. Two points virtual extensometers were applied in this phase. Experimental results were then compared to the reference $da/dN - \Delta K_{eff}$ curve: it was found that the correct estimation of crack opening levels shifts all the experimental points on the reference curve, showing that DIC can be successfully applied to measure crack closure effects.

KEYWORDS. Fatigue crack growth; Haynes 230; Crack closure; Effective stress intensity factors; Digital image correlation.

INTRODUCTION

The continuously increasing demand of electrical power, together with the necessity to provide energy in a more sustainable way, has led to a renewed interest in nickel-based superalloys. This is mainly related to the fact that these materials exhibit an excellent resistance to high temperature and corrosion, features that make them the preferable choice for components working in harsh environments, like those present in the combustion chambers of gas turbines. In this paper, fatigue crack growth of a commercially available nickel-based superalloy, Haynes 230, is investigated. Room temperature conditions are taken into account, in order to measure fatigue crack growth with optical methods, avoiding the effects of further damage mechanisms, like oxidisation.

In 1970, Elber[1] discovered the phenomenon of plasticity induced crack closure and proposed to modify the Paris equation, by replacing ΔK with the effective stress intensity factor range, ΔK_{eff}, computed considering only the portion of the load cycle where the crack stays open. This modification removed the dependency of crack growth rates on R, demonstrating that crack closure plays an important role in fatigue and that only a parameter can be used to describe Mode I propagation. In this work, ΔK_{eff} is extracted from the singular field present at the tip of a fatigue crack.

A crack tip can be modelled as singularity point in the stress and strain fields of a cracked body. Williams[2] analytically described the stress field present at the tip of a crack in an elastic and isotropic body with an infinite power series. Williams found the singularity at the tip to be of the $r^{-1/2}$ order, where r is the radial distance from the crack tip, and that stress intensity factors are a measure of the singularity itself. In this work the analytical solution provided by Williams was fitted with the experimental displacements measured by digital image correlation (DIC).

DIC was originally applied to fatigue crack growth to measure crack closure effects [3, 4]. Local measurements of crack tip opening levels were initially obtained with two points digital extensometers, following Elber's proposal[1, 5]. McNeill *et al.*[6] were the first to propose to extract stress intensity factors from DIC-measured displacements. The necessity to

introduce the second term of William's expansion, the T-stress, was highlighted by Carroll *et al.* in [7]. Recently, DIC was employed to analyse fatigue crack growth at high temperature in Haynes 230[8]. In a study of fatigue crack growth in Haynes 230 single crystals[9], DIC was employed to extract effective stress intensity factor ranges during mixed mode propagation in an anisotropic body. An interesting feature of these techniques was that they allow the direct determination of the effective stress intensity factor range. ΔK_{eff}, since the effects of plasticity induced crack closure are inherently included in the experimental displacements.

In this work, state of the art procedures are applied, in order to provide a deep analysis of fatigue crack growth, mainly focusing on the differences between local and global measurement techniques. In the first part of the paper material properties are discussed. This section is followed by a description of the experiments and an overview of the DIC procedures employed during the tests. Finally, the results provided by full field regression algorithms are initially presented and then compared to the crack closure measurements provided by local methods based on virtual extensometers.

MATERIALS

Haynes 230 is a solid solution strengthened superalloy, usually employed for gas turbines and aerospace applications, since it exhibits high resistance to oxidation and creep. High temperature properties of Haynes 230 are due to the additions of chromium, tungsten and molybdenum. The chemical composition of the alloy employed for testing is reported in Tab. 1.

Al	B	C	Co	Cr	Cu	Fe	La	Mn
0.35	0.005	0.1	0.16	22.14	0.04	1.14	0.015	0.5
Mo	Ni	P	S	Si	Ti	W	Zr	
1.25	Bal.	0.005	0.002	0.49	0.01	14.25	0.01	

Table 1: Chemical composition (%wt) of Haynes 230.

Specimens were obtained from a round bar, whose diameter was 38 mm. Before testing, a portion of the bar was etched, in order to observe Haynes 230 microstructure, which is reported in Fig. 1. It was found that the typical microstructure has a wide range of grain sizes: the average grain size, calculated following the procedure outlined in ASTM E112, was found to be about 54 μm. It is also worth remarking that a large amount of twins are present in the alloy together with a large number of tungsten carbides (the dark spots in Fig. 1).

EXPERIMENTS

Two series of tests were carried out: in order to obtain a reference $da/dN - \Delta K$ curve, two fatigue crack growth tests were performed on single edge bending (SE(B)) specimens. These experiments were carried out following the compression-precracking procedures discussed in ASTM E647 standard. A load ratio equal to 0.7 was employed in this phase, in order to obtain a closure-free propagation curve. During the experiments, the load frequency was fixed at 10 Hz.

The first experiment was performed, after compression precracking, following the constant amplitude (CPCA) procedure, to investigate the steady state region of crack growth, also known as region II propagation: experimental data were fitted with the Paris law, whose coefficients are reported in Fig 2.

The second test was performed following the ΔK-decreasing procedure, in order to evaluate the fatigue threshold. This experiment was terminated when a crack growth rate equal to 10^{-10} m/cycle was observed. It was found that the fatigue threshold of Haynes 230 at room temperature is equal to 5.8 MPa√m. In order to obtain a unique curve for both the experiments, they were fitted with the NASGRO equation [10], which was modified to take into account that only one load ratio was investigated:

$$\frac{da}{dN} = c \left(\Delta K_{R=0.7} \right)^{m} \left(1 - \frac{\Delta K_{th}}{\Delta K_{R=0.7}} \right)^{p} \tag{1}$$
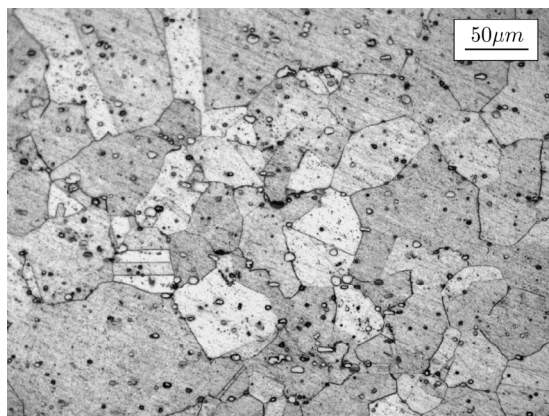
Figure 1: Microstructure of the as-received Haynes 230 material showing twins and a wide range of grain sizes, together with a large number of carbides.

The second series of experiments was performed on single edge dogbone specimens. Notches were made by electrical discharge machining (EDM). Specimens gage length, width and thickness are reported, together with notch depth, in Fig. 3, where a schematic of specimen geometry is reported.

Before testing specimens were accurately prepared. Measurement surfaces were mechanically polished to a mirror finish with abrasive paper, up to a grit of P2500. A speckle pattern, necessary for digital image correlation, was airbrushed on each specimen using black paint. An airbrush with a 0.18 mm wide needle was employed in this phase: this was necessary to obtain a refined pattern, necessary for high quality measurements. Images were acquired by an high definition digital camera, whose resolution was 2048 x 1536 pixels. A magnification of 3X, obtained using an adjustable lens with a 6.5X magnification range and a 10X adapter, was employed during the experiments. This setup allowed a resolution of 0.94 pixel/μm. the experimental setup is shown in Fig. 3.

Specimens were cyclically loaded in a servo-hydraulic load frame at the load ratios R and stress ranges, $\Delta\sigma$, given in Tab. 2. A frequency equal to 10 Hz was employed during the experiments. Once a crack was visually identified, measurement cycles were run periodically to capture a higher number of pictures, necessary to provide a more accurate analysis of the fatigue process.
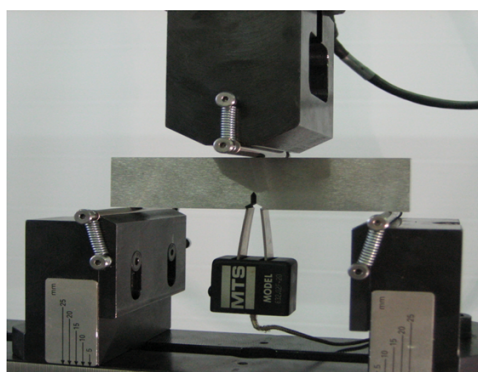
(a)
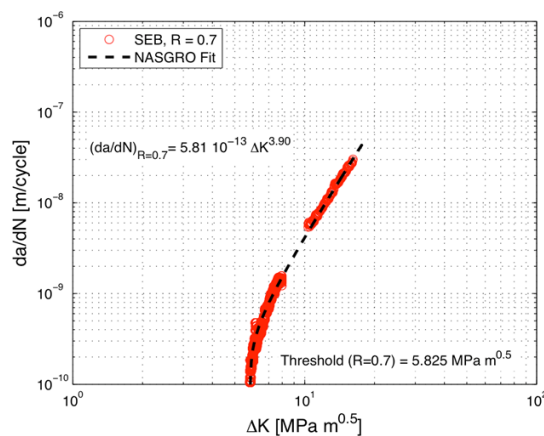
(b)

Figure 2: Fatigue crack growth tests at room temperature on SE(B) specimens. (a) SEB specimen mounted in the three point bending fixture; (b) experimental results.

Specimen #	Stress ratio R	$\Delta\sigma$ [MPa]	Images per cycle
1	0.1	180	33
2	0.1	140	39
3	-1	240	39

Table 2: Summary of the fatigue crack growth test parameters.
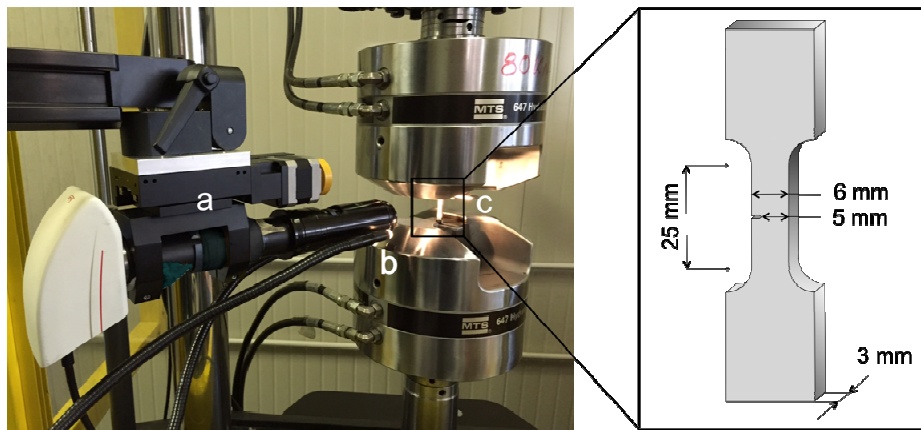
Figure 3: The experimental setup and a schematic of specimen geometry: a) HD digital camera and lens; b) light source and c) specimen mounted in the load-frame.
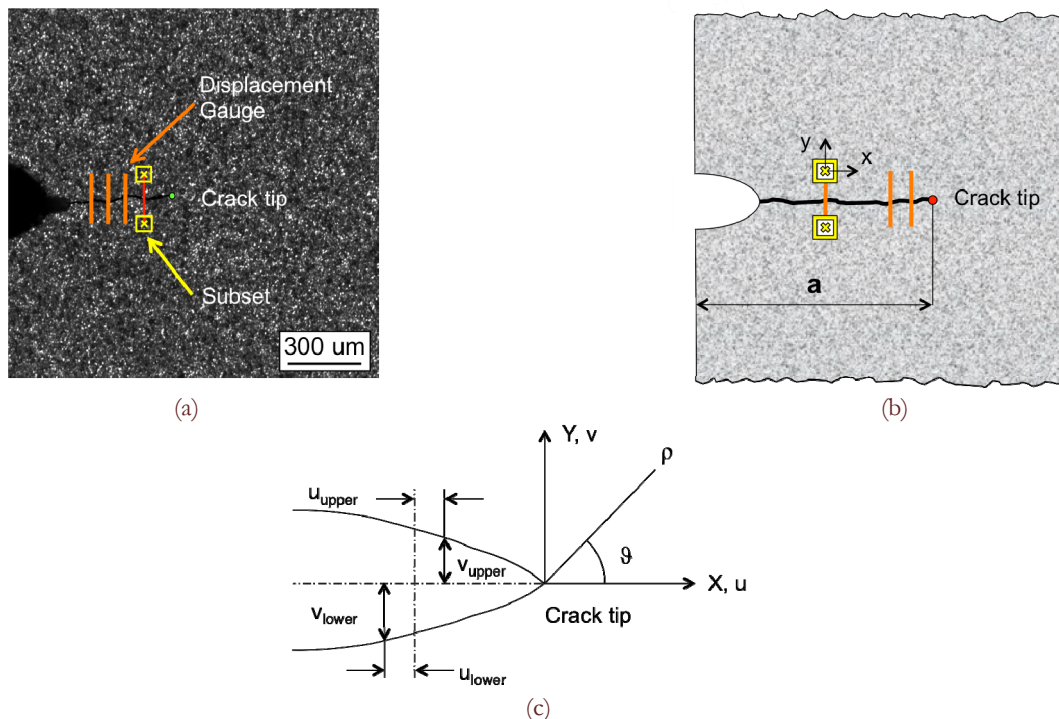

(a)

(b)

(c)

Figure 4: (a) An example of virtual-extensometers disposition on a specimen. (b) A schematic showing the displacements measured by extensometers. (c) Coordinate system for measuring crack opening and sliding displacements [11].

DIGITAL IMAGE CORRELATION PROCEDURE

The displacement fields measured by DIC are the starting point of the analysis developed in this study. DIC determines the displacements by tracking the different positions of the speckles present on the measurement surfaces. Square groups of pixels, usually defined subsets, are tracked to get the best correlation between two different images.

DIC analysis was performed using Vic 2D, a commercially available correlation software. The reference image, the picture from which all the relative displacements are calculated, was taken when the minimum stress was applied, at the beginning of each measurement cycle. Full field images were correlated to get both horizontal and vertical displacements, considering not only the points before, but also those beyond the crack tip. The dimension of the square subsets was fixed during the analysis and was equal to 51 pixels.

Two points virtual extensometers were adopted to observe crack opening loads, as shown in Fig. 4a and b. Several virtual extensometers were placed along the crack profile, in order to observe the evolution of crack profile during a fatigue cycle. Virtual extensometers were positioned perpendicular to the crack plane: this was necessary to get pure vertical displacements, necessary to evaluate crack opening levels. The difference in the vertical crack tip displacements (Fig. 4c), $\Delta v = v_{upper} - v_{lower}$, was employed to describe Mode I opening.

CRACK CLOSURE MEASUREMENTS BASED ON FULL FIELD REGRESSION

DIC allows the evaluation of the singular displacement field that surrounds a crack tip. This field can be used to evaluate crack propagation driving forces without geometric considerations. A nonlinear least-squares regression algorithm can be used to extract the effective stress intensity factor ranges, ΔK_{eff}, starting from DIC displacements. Moreover, taking several pictures of the defect during a load cycle, is it possible to evaluate the evolution of ΔK_{eff} and to calculate crack opening levels. In this work, the procedure discussed in [7-9, 11] is adopted.

Since no mode II sliding was observed, since the crack propagated in a plane perpendicular to the loading direction, only ΔK_I was considered in the calculations. For a pure Mode I loaded crack in an isotropic body, the vertical displacement field is expressed as [2]:

$$v = \frac{\Delta K_I}{\mu}\sqrt{\frac{\rho}{2\pi}}\sin\left(\frac{\vartheta}{2}\right)\left[\frac{1}{2}(\kappa+1)-\cos^2\left(\frac{\vartheta}{2}\right)\right]-\frac{1}{2\pi}\left(\frac{\nu}{1+\nu}\right)T\rho\sin(\vartheta)+A\rho\cos(\vartheta)+B \qquad (2)$$

where ρ and ϑ are the coordinates of the points surrounding the tip, expressed in the cylindrical reference system proposed in Fig. 4c, μ is the shear modulus, T is the T-stress, the second term of Williams' expansion, A and B are two terms that take into account rigid body rotation and translation and κ is given by:

$$\kappa = \frac{3-\nu}{1+\nu} \qquad (3)$$

since plane stress conditions are taken into account.

In Fig. 5a, vertical displacements, measured by DIC around the tip of a 1.8 mm long crack subjected to a stress ratio equal to 0.1, are reported. Regression algorithm was applied on these displacements: initially, a 0.36 mm² wide area was considered. In Fig. 5b, the comparison between experimental and analytical results is reported: the displacements calculated by regression, represented in the figure by a red line, are in good agreement with those experimentally measured (blue contours of the figure). The value of $\Delta K_{I,eff}$, calculated by the regression algorithm was equal to 24.7 MPa√mm.

In order to estimate crack closure effect, this value should be compared to the total stress intensity factor range ΔK_I. This value can be analytically calculated:

$$\Delta K_I = Y\Delta\sigma\sqrt{\pi a} \qquad (4)$$

where a is the crack length and Y is a factor that accounts for specimen geometry, calculated as expressed in Eq.5 [12], where W is specimen width.

$$Y = 0.265(1-a/W)^4 + \frac{0.857+0.265(1-a/W)}{(1-a/W)^{3/2}} \qquad (5)$$

For the given configuration, it results that $\Delta K_I = 25.2$ MPa√m. The effective stress intensity ratio U, defined by Elber [1, 5] as the ratio between $\Delta K_{I,eff}$ and ΔK_I, in this case is equal to 0.98, meaning that the crack stays open for 98% of the fatigue cycle. This value does not agree with the other measurements present in the literature[13]: this can be related to a wrong estimation of $\Delta K_{I,eff}$. In particular, it was found that the value of ΔK_I strongly depends on the extension of the area considered in regression calculations. In order to take into account only the singular field and to avoid the effects related to the remote loading conditions, a small area, whose extension was 0.07 mm², was considered. It was found that the value of $\Delta K_{I,eff}$ drastically decreases till a value of 15.3 MPa√m. This means that U lowers to 0.61, a value which is similar to those presented in the literature for the given loading conditions. In Fig. 5c, the evolution of $\Delta K_{I,eff}$ during a fatigue cycle is reported: the value of the effective stress intensity factor range is equal to zero when the crack stays closed, whereas it begins to increase when the crack starts opening. It is worth remarking that the trend between the applied stress range and $\Delta K_{I,eff}$ is not linear: this is related to material elastic-plastic behavior.
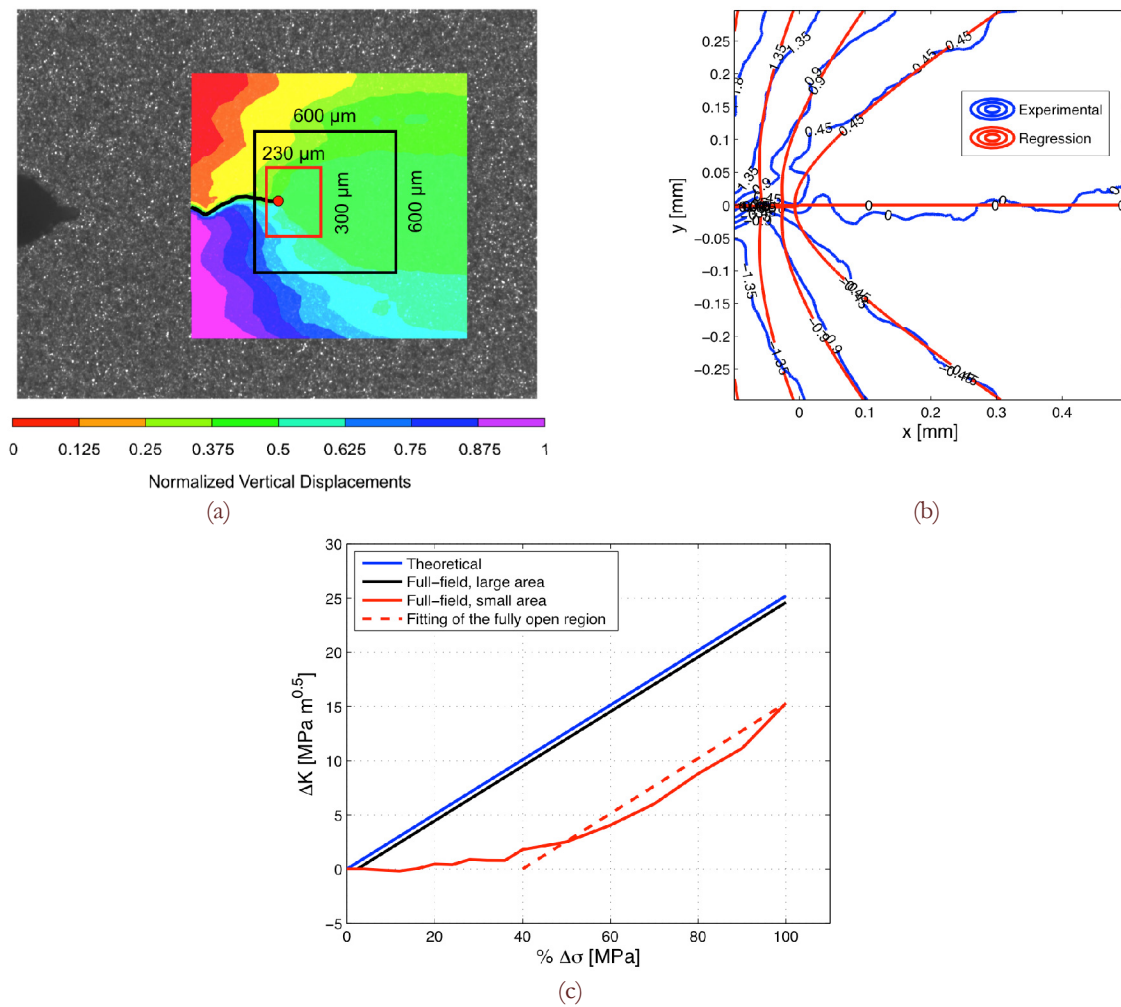
(a)

(b)

(c)

Figure 5: DIC analysis of a 1.8 mm long defect subjected to a stress ratio equal to 0.1 (a) DIC measured vertical displacements around the tip, together with the extension of the two areas of regression selected for the analysis. (b) comparison between experimental and analytical displacements; (c) the evolution of the effective stress intensity factor range during a fatigue cycle for the two selected areas of regression.

CRACK CLOSURE MEASUREMENTS WITH TWO POINTS VIRTUAL EXTENSOMETERS

Horizontal and vertical displacements were recorded for each virtual extensometer during the fatigue cycle. Since no Mode II sliding was observed in all the considered specimens, only vertical displacements around crack tip were considered. The measured vertical displacements for the defect analysed in the previous section, are provided in Fig. 6a, where it can be seen that the crack starts opening from the notch at 24% of the applied stress range. At this point the crack tip is still closed: opening is evident at 50% of the applied stress range.

The dependency of local crack opening levels on the distance from crack tip was investigated by considering three virtual extensometers placed at 50, 150 and 300 μm from the tip, as reported in Fig 6b, c and d. Crack opening was evaluated by fitting the portion of the COD vs Δσ plot in which the crack is fully open, as suggested in [14]. The opening load was defined as the stress level of the fitting line when the COD is equal to 0. It was found that crack opening levels are increasing when extensometers nearer to the tip are taken into account. This behavior is expected since cracks generally open first at the mouth and last at the crack tip.

In order to correctly evaluate the value of the opening load, only a COD was considered during the calculations: it was chosen to extract the opening levels by considering the closest extensometer to the tip that gave back measurements without noise. It was found that this condition was obtained by considering the COD placed at 50 μm from the tip.

It can be noted that the value of U calculated from regression is higher than the one evaluated by the extensometer placed 50 µm behind the tip. This is due to the fact that regression considers not only the points near the tip, but also those far from the defect, giving back an average estimate of the opening levels. This trend was also confirmed in another study, in which fatigue crack growth in Haynes 230 single crystals was investigated [15]. Therefore, in the following calculations only the opening levels calculated with virtual extensometers will be taken into account, since they have proven to provide better estimates.
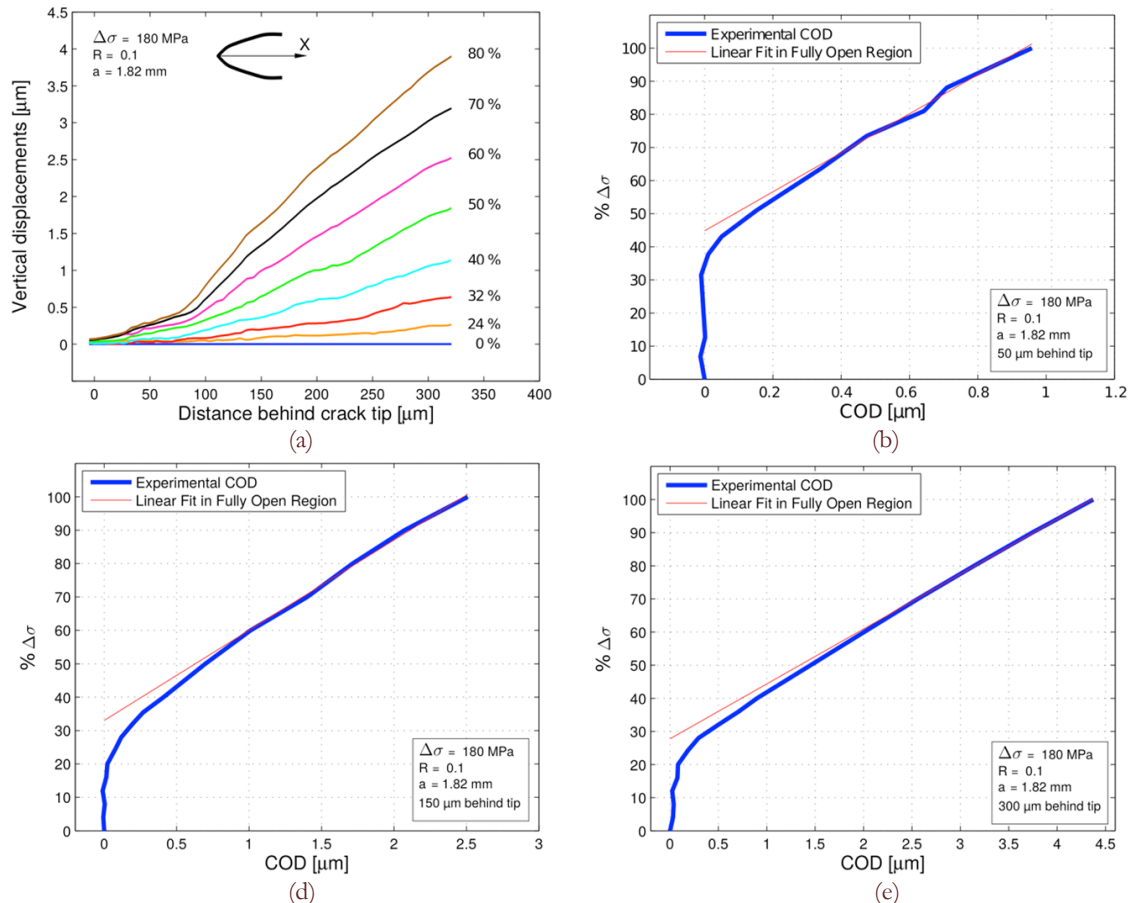

Figure 6: (a) The vertical crack opening displacement profile of the specimen loaded at R=0.1 and $\Delta\sigma = 180$ *MPa* with a measured crack length of 1.82 mm; (b) COD vs $\Delta\sigma$ measured at 50 µm from the tip; (c) COD vs $\Delta\sigma$ measured at 150 µm from the tip; (d) COD vs $\Delta\sigma$ measured at 300 µm from the tip.

Two selected COD for the two different load ratio investigated are reported in Fig. 7a and c: the method is consistent and provides accurate estimations. Experimental results, expressed in terms of U = $\Delta\sigma_{\text{eff}}$ / $\Delta\sigma$ are reported in Fig. 7b and d: small scatter is observed between the two specimens tested at R = 0.1. It was found that a crack, when a R = 0.1 test is considered, stays open for 47% of the fatigue cycle, whereas the crack subjected to fully reversed loading is open only for 30% of the applied stress range.

STRESS INTENSITY FACTOR RANGES AND CRACK GROWTH CURVE EVALUATION

Experimental results are compared to the reference $da/dN - \Delta K_{I,eff}$ curve in Fig. 8a in terms of the total stress intensity factor range: as expected, crack growth rates are strongly dependent on the applied load ratio. In order to remove the dependency on R, effective stress intensity factor ranges, $\Delta K_{I,eff}$ were calculated as proposed in Eq. 6, where U is the effective stress intensity factor ratio, experimentally calculated as proposed in Fig. 7.

$$\Delta K_{I,eff} = U \cdot \Delta K_I \tag{6}$$

The adoption of experimentally measured opening levels, as reported in Fig. 8b, removes the influence of R from the experimental results and moves all the experimental data-points on the reference $da/dN - \Delta K_{eff}$ curve. It is also worth remarking that this fact confirms the experimental observations with DIC and underlines the accuracy of the method based on virtual extensometers.
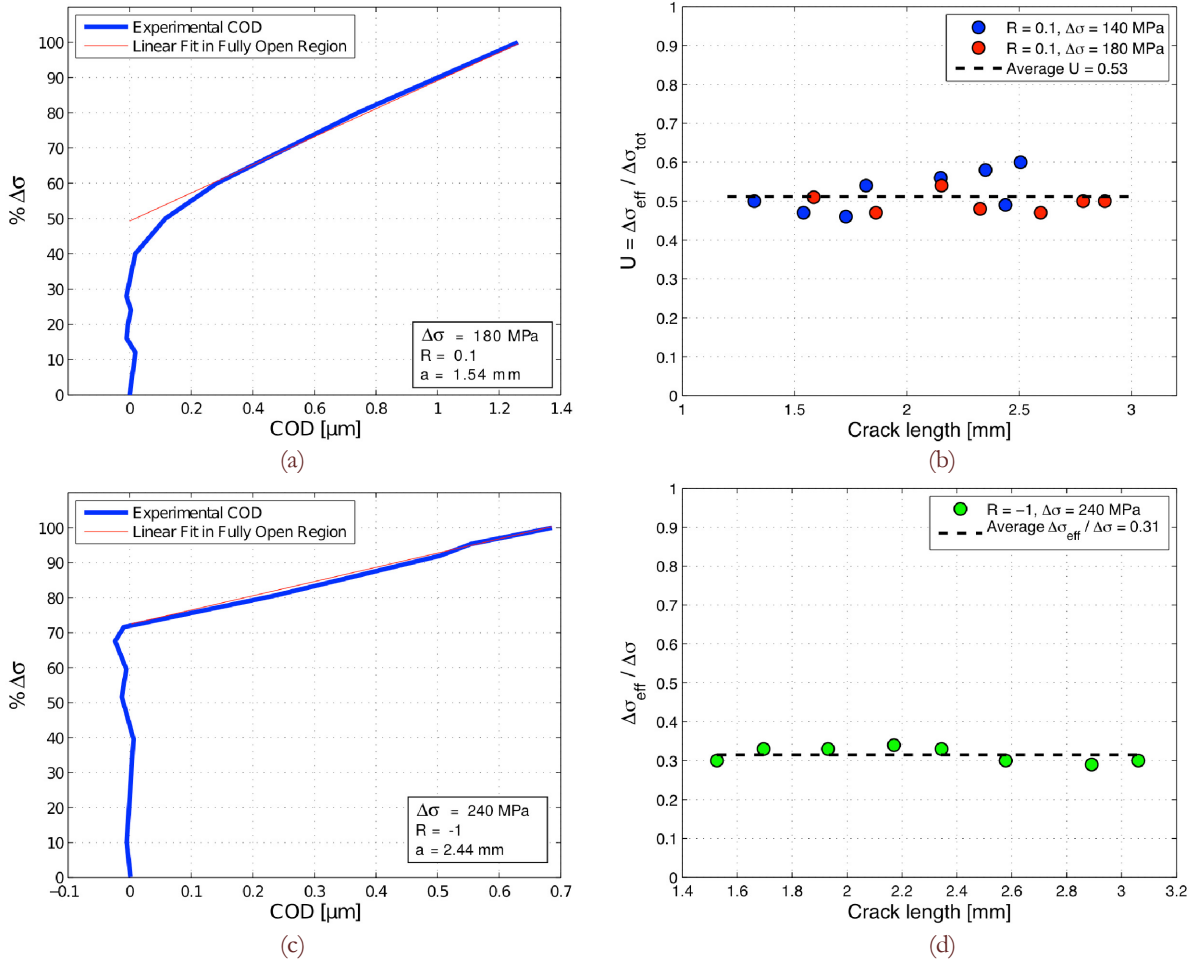

Figure 7: Crack opening measurements with DIC. (a) and (c) selected COD vs $\Delta\sigma$ behavior for the two considered loading conditions; (b) and (d) crack closure evolution during fatigue tests.
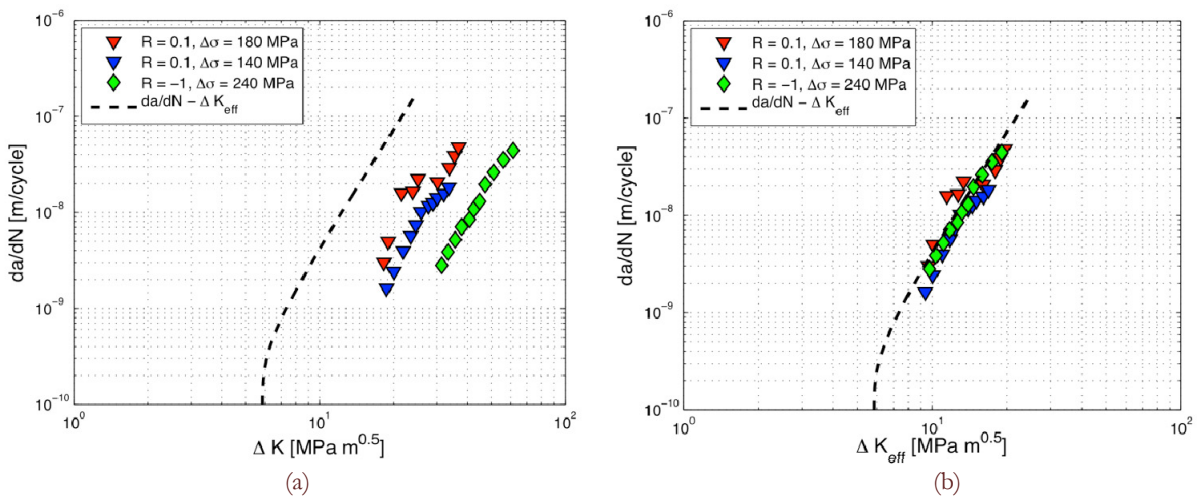

Figure 8: Fatigue crack growth results. (a) experimental results in terms of da/dN vs ΔK; (b) experimental results in terms of da/dN vs ΔK_{eff}.

CONCLUSIONS

Fatigue crack growth in Haynes 230 was investigated at room temperature. Digital image correlation was employed to calculate crack opening levels. Two different approaches were applied to evaluate crack opening levels: it was found that crack closure measurements based on regression algorithms are strongly dependent on the extension of the regression areas. A more accurate estimation of crack closure effects was obtained by applying two points virtual extensometers. It was found that crack opening levels are changing along the crack profile: in order to obtain a more accurate closure measurement, opening levels were evaluated by placing a virtual extensometer 50 μm behind the crack tip. This distance was found to be the closest capable of providing noiseless results. The accuracy of the measurements was verified in terms of crack growth: the calculation of the effective stress intensity factor ranges, based on experimental opening levels, removed the dependency of crack growth rates on the applied stress ratios, underlining the fact that DIC can be successfully applied to fatigue crack growth. Similar measurements are being carried out on single crystals of the same material, in order to compare the closure levels at the same ΔK levels, between single and polycrystals.

REFERENCES

[1] Elber, W., Fatigue crack closure under cyclic tension. Engineering Fracture Mechanics, 2(1) (1970) 37-45.
[2] Williams, M.L., On stress distribution at base of stationary crack. American Society of Mechanical Engineers - Transactions - Journal of Applied Mechanics, 24(1) (1957) 109.
[3] Riddell, W.T., et al., Determining fatigue crack opening loads from near-crack-tip displacement measurements. ASTM STP, 1343 (1999) 157.
[4] Sutton, M.A., et al., Local crack closure measurements: Development of a measurement system using computer vision and a far-field microscope. ASTM STP, 1343 (1999) 145.
[5] Elber, W. The significance of fatigue crack closure. in Damage Tolerance in Aircraft Structures: A Symposium. In: Seventy-third Annual Meeting American Society for Testing and Materials, Toronto, Ontario, Canada, 21-26 June 1970.. ASTM International. (1971).
[6] McNeill, S.R., W.H. Peters, and M.A. Sutton, Estimation of stress intensity factor by digital image correlation. Engineering Fracture Mechanics, 28(1) (1987) 101.
[7] Carroll, J., et al., Investigation of fatigue crack closure using multiscale image correlation experiments. Engineering Fracture Mechanics, 76(15) (2009) 2384.
[8] Pataky, G.J., H. Sehitoglu, and H.J. Maier, High temperature fatigue crack growth of Haynes 230. Materials Characterization, (2012).
[9] Rabbolini, S., et al., Fatigue crack growth in Haynes 230 single crystals: an analysis with digital image correlation. Fatigue & Fracture of Engineering Materials & Structures, (2014).
[10] Forman, R.G., Mettu, S.R., Behavior of surface and corner cracks subjected to tensile and bending loads in Ti-6Al-4V alloy. (1990).
[11] Pataky, G.J., et al., Full field measurements of anisotropic stress intensity factor ranges in fatigue. Engineering Fracture Mechanics, 94 (2012) 13-28.
[12] Tada, H., P.C. Paris, Irwin, G.R., The analysis of cracks handbook.: New York: ASME Press, (2000).
[13] Schijve, J., Fatigue crack closure: observations and technical significance, in Mechanics of fatigue crack closure, American Society for Testing and Materials Philadelphia, PA., (1988) 5-34.
[14] Allison, J.E., R.C. Ku, Pompetzki, M.A., A comparison of measurement methods and numerical procedures for the experimental characterization of fatigue crack closure. Mechanics of fatigue crack closure, ASTM STP, 982 (1988) 171-85.
[15] Rabbolini, S., S. Beretta, Sehitoglu, H., Fatigue crack growth in Haynes 230: a comparison between single crystals and polycrystal effective curve, in 15th International ASTM/ESIS Symposium on Fatigue and Fracture Mechanics: Anaheim, CA, USA (2015).